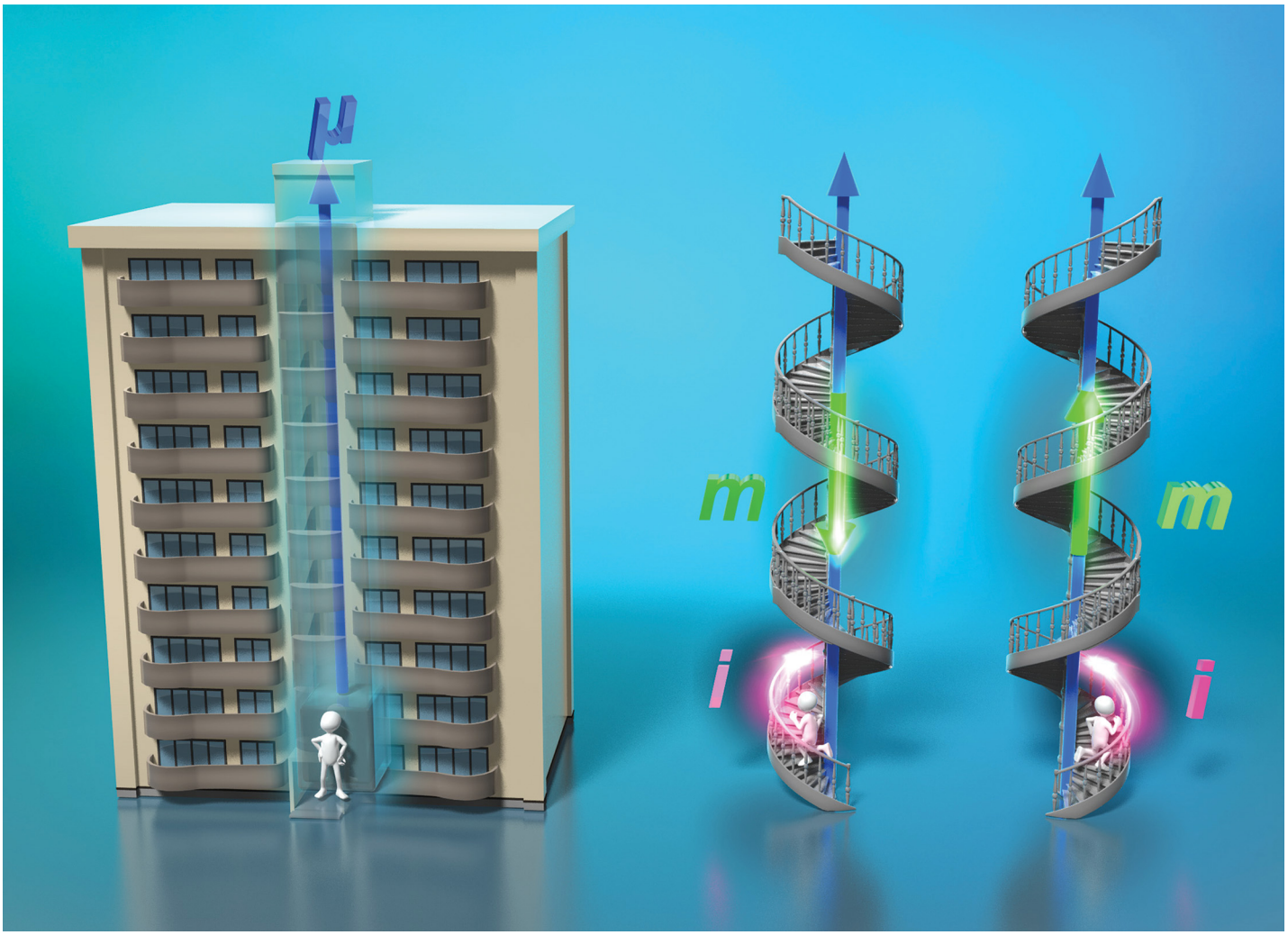

Showcasing research from the Group of Dr Ayumi Imayoshi and Prof. Kazunori Tsubaki at Kyoto Prefectural University

Inversion of circularly polarized luminescence by electric current flow during transition

This study proposes a methodology for predicting the magnetic transition dipole moment (*m*), critical for CPL activity, directly from molecular structures by focusing on the instantaneous current (*i*) during transitions. A classical loop model explains the CPL sign inversion caused by differences in substitution positions. If the electric dipole moment (μ) represents the "difference" in electron presence during transitions, like the directionality of taking an elevator upward, *m* reflects the "path" of electron flow, like the rotation of ascending a spiral staircase.

As featured in:

See Ayumi Imayoshi, Kazunori Tsubaki *et al.*, *Phys. Chem. Chem. Phys.*, 2025, **27**, 77.

ROYAL SOCIETY OF CHEMISTRY

rsc.li/pccp

Registered charity number: 207890

PCCP Owner Societies

PCCP

ROYAL SOCIETY OF CHEMISTRY

PAPER

View Article Online
View Journal | View Issue

Cite this: *Phys. Chem. Chem. Phys.*, 2025, **27**, 77

Inversion of circularly polarized luminescence by electric current flow during transition†

Ayumi Imayoshi, *[a] Shinya Fujio,[a] Yuuki Nagaya,[a] Misato Sakai,[a] Atsushi Terazawa,[a] Misa Sakura,[a] Keita Okada,[b] Takahiro Kimoto,[b] Tadashi Mori,[c] Yoshitane Imai,[b] Masahiko Hada[a] and Kazunori Tsubaki *[a]

The development of chiral compounds exhibiting circularly polarized luminescence (CPL) has advanced remarkably in recent years. Designing CPL-active compounds requires an understanding of the electric transition dipole moment (μ) and the magnetic transition dipole moment (m) in the excited state. However, while the direction and magnitude of μ can, to some extent, be visually inferred from chemical structures, m remains elusive, posing challenges for direct predictions based on structural information. This study utilized binaphthol, a prominent chiral scaffold, and achieved CPL-sign inversion by strategically varying the substitution positions of phenylethynyl (PE) groups on the binaphthyl backbone, while maintaining consistent axial chirality. Theoretical investigation revealed that the substitution position of PE groups significantly affects the orientation of m in the excited state, leading to CPL-sign inversion. Furthermore, we propose that this CPL-sign inversion results from a reversal in the rotation of instantaneous current flow during the $S_1 \rightarrow S_0$ transition, which in turn alters the orientation of m. The current flow can be predicted from the chemical structure, allowing anticipation of the properties of m and, consequently, the characteristics of CPL. This insight provides a new perspective in designing CPL-active compounds, particularly for C_2-symmetric molecules where the $S_1 \rightarrow S_0$ transition predominantly involves LUMO → HOMO transitions. If μ represents the directionality of electron movement during transitions, *i.e.*, the "difference" in electron locations before and after transitions, then m could be represented as the "path" of electron movement based on the current flow during the transition.

Received 27th July 2024,
Accepted 8th November 2024

DOI: 10.1039/d4cp02968b

rsc.li/pccp

Introduction

Circularly polarized luminescence (CPL) has attracted significant interest in recent years owing to, alongside its potential applications,[1] its ability to provide insights into the structure–property relationship of molecules in their excited states. The binaphthyl motif has emerged as a prominent scaffold for integrating chiral elements, and numerous chiral binaphthyl derivatives exhibiting robust CPL have been documented,[2–6] including its uses as additives,[7,8] ligands[9] and polymers.[10]

Theoretically, the sign of CPL is expected to reverse upon the introduction of a chiral element with an opposite configuration. However, binaphthyls with identical axial handedness can also invert their chiroptical properties, depending on factors such as the dihedral angle (ϕ) between the binaphthyl units or the structure of the linker in the binaphthol's hydroxy groups.[11] Takaishi and Ema *et al.* demonstrated through computational investigations that the CPL sign of (*S*)-1,1′-binaphthyl reverses at a dihedral angle of around 90°.[12]

The sign of CPL can be inverted not only through structural modifications[5,6,13] but also by varying the environmental conditions of the molecule,[14] such as solvent[3,15] and temperature.[4,8] This inversion occurs while maintaining the same handedness in the binaphthyl core. However, a deeper understanding of the relationship between these chemical structures and the CPL sign remains elusive, particularly regarding the electronic (μ) and magnetic (m) transition dipole moments crucial for enhancing the dissymmetry (g_{lum}) value. This value is defined as 2 $(I_L - I_R)/(I_L + I_R)$, where I_L and I_R represent the intensity of left and right-handed CPL, respectively. Especially challenging is the prediction of the properties of the magnetic (m) moment from chemical structures, a methodology that is critically needed.[16]

[a] *Graduate School of Life and Environmental Sciences, Kyoto Prefectural University, 1-5 Hangi-cho, Shimogamo, Sakyo-ku, Kyoto 606-8522, Japan. E-mail: imayoshi@kpu.ac.jp, tsubaki@kpu.ac.jp*
[b] *Department of Applied Chemistry, Faculty of Science and Engineering, Kindai University, 3-4-1 Kowakae, Higashi-Osaka, Osaka 577-8502, Japan*
[c] *Department of Applied Chemistry, Graduate School of Engineering, Osaka University, 2-1 Yamada-oka, Suita, Osaka 565-0871, Japan*

† Electronic supplementary information (ESI) available. See DOI: https://doi.org/10.1039/d4cp02968b

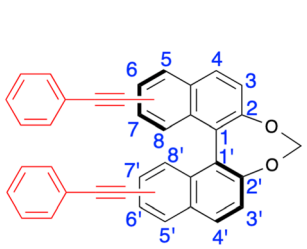

compound	g_{lum} (exp)
(*S*)-**3-PE$_1$**	−1.5 × 10^{-3}
(*S*)-**4-PE$_1$**	−0.52 × 10^{-3}
(*S*)-**5-PE$_1$**	−1.9 × 10^{-3}
(*S*)-**6-PE$_1$**	−1.8 × 10^{-3}
(*S*)-**7-PE$_1$**	+5.6 × 10^{-3}
(*S*)-**8-PE$_1$**	−1.8 × 10^{-3}

Fig. 1 Summary of our recent study[17] on methylene-linked binaphthol derivatives (*S*)-**3-PE$_1$** to (*S*)-**8-PE$_1$** with phenylethynyl (PE) groups at from 3,3′ to 8,8′ positions on the binaphthyl backbone and their dissymmetry (g_{lum}) values for CPL.

Recently, we reported a complete series of binaphthyl derivatives with a methylene tether, incorporating phenylethynyl (PE) groups at the 3,3′- to 8,8′-positions of a 1,1′-bi-2-naphthol backbone (**3-PE$_1$** to **8-PE$_1$**). Among these, only **7-PE$_1$** exhibited a reversal in the CPL sign (Fig. 1).[17] In this study, we specifically focused on **7-PE$_1$** and **6-PE$_1$**, which exhibit positive and negative CPL, respectively, to elucidate the details behind these observations.

Results and discussion

We performed further CPL studies on binaphthyl derivatives with varied tether groups and PE-substitution locations. The binaphthol derivatives **7-PE$_n$** and **6-PE$_n$** feature free methoxy groups (n = Me) or are connected by methylene, ethylene, and propylene chains (n = 1, 2, or 3, represented as –$(CH_2)_n$–) along with a –$CH_2C{\equiv}CCH_2$– linker (n = butyne) (Fig. 2a). This systematic alteration affects the dihedral angle between the naphthalenes (**7-PE-Naph** and **6-PE-Naph**) in their ground (ϕ_g) and excited (ϕ_{ex}) states. The former was promptly confirmed by density functional theory (DFT) calculations at the B3LYP/6-31G(d,p) level (Fig. 2b).

Fig. 3a–d shows the fluorescence (FL) and CPL spectra of **7-PE$_n$** and **6-PE$_n$** in chloroform. To ensure clarity, axial chirality throughout this study consistently refers to the (*S*)-configuration for both **7-PE$_n$** and **6-PE$_n$**. Among the derivatives of **7-PE$_n$** and **6-PE$_n$** (n = 1, 2, 3, Me, and butyne), the methylene-tethered binaphthyls **7-PE$_1$** and **6-PE$_1$**, featuring the smallest dihedral angles, exhibit distinct fluorescence behavior characterized by low-energy and broad emissions at λ_{max} = 407 and 398 nm, respectively. Both the CPL signals of **7-PE$_1$** and **6-PE$_1$** have higher intensities compared with derivatives having other linker groups,[18] with substantial g_{lum} values of +5.6 × 10^{-3} and −1.8 × 10^{-3}, respectively. The **7-PE$_n$** series tends to consistently exhibit higher g_{lum} values compared with the **6-PE$_n$** series with identical linkers,[19] as depicted in Fig. 3e. Interestingly, the g_{lum} values for **7-PE$_n$** are more affected by the linker groups, while **6-PE$_1$** shows a significantly higher g_{lum} value in the **6-PE$_n$** series.

The main distinction between **7-PE$_n$** and **6-PE$_n$** derivatives lies in the inherent difference in the CPL sign, despite having the same axial chirality (compare Fig. 3a and c). Thus, all (*S*)-**7-PE$_n$** compounds exhibited CPL with positive (+) signs, while all

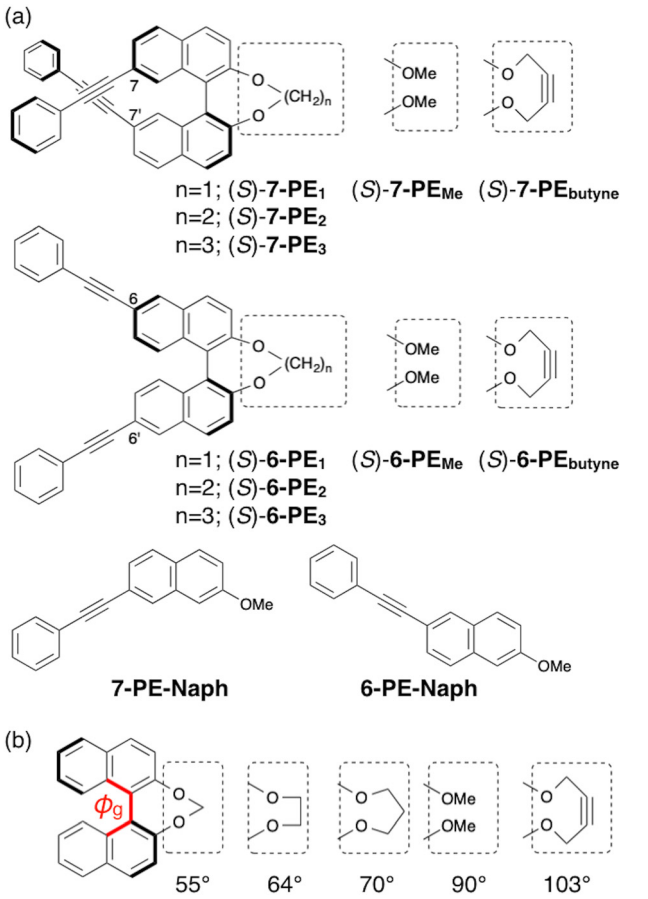

Fig. 2 (a) Structures of binaphthol derivatives **7-PE$_n$** and **6-PE$_n$**, along with their naphthalene (Naph) units. (b) Variation of dihedral angles between naphthalene rings in the ground state (ϕ_g) calculated at the B3LYP/6-31G(d,p) level.

(*S*)-**6-PE$_n$** compounds exhibited CPL with negative (−) signs, regardless of their respective linker groups. In essence, the inversion of CPL sign was achieved solely by altering the PE-substitution positions on the binaphthyl backbone.

To better understand the origin of this sign inversion, theoretical investigations were conducted as follows:[20] The chiroptical and structural computations for **7-PE$_1$** and **6-PE$_1$** in their excited states were initially performed using the TD-DFT approach, which successfully reproduced the observed trends, including the CPL-sign inversion (Table S2, ESI†). To enhance the accuracy of our calculations, we subsequently employed time-dependent approximate coupled cluster calculations at the RI-CC2/def2-TZVP level[21] for **7-PE$_1$** and **6-PE$_1$**.

Table 1 shows a comparison between the calculated and experimental g_{lum} values as derived from the optimized excited state structures. While slightly larger discrepancies were observed for **7-PE$_1$**, the calculated values successfully reproduce the trends in both intensity and sign of the g_{lum} value.

Crucial structural features relevant to the electronic transitions are also summarized in Table 1. The dihedral angles between the binaphthyl units are lower in the excited state (ϕ_{ex}) compared with the ground state (ϕ_g). This structural

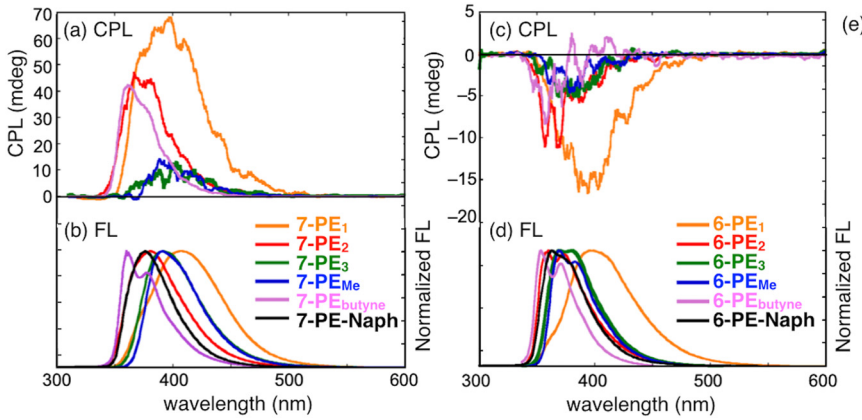

(e)

compound	λ_{em} (nm)	g_{lum} (exp)
7-PE$_1$	407	5.6 × 10^{-3}
7-PE$_2$	381	3.2 × 10^{-3}
7-PE$_3$	392	0.68 × 10^{-3}
7-PE$_{Me}$	391	0.88 × 10^{-3}
7-PE$_{butyne}$	354, 377	3.04 × 10^{-3}
7-PE-Naph	373	–
6-PE$_1$	398	−1.8 × 10^{-3}
6-PE$_2$	360, 373	−0.78 × 10^{-3}
6-PE$_3$	370, 381	−0.50 × 10^{-3}
6-PE$_{Me}$	369, 383	−0.58 × 10^{-3}
6-PE$_{butyne}$	354, 370	−0.49 × 10^{-3}
6-PE-Naph	363	–

Fig. 3 (a) CPL spectra of **7-PE$_n$**. Conditions: 1.0 × 10^{-5} M in $CHCl_3$, 25 °C. λ_{ex} = 280 nm (**7-PE$_1$**, **7-PE$_2$**, **7-PE$_3$**, **7-PE$_{Me}$**), 278 nm (**7-PE$_{butyne}$**). (b) FL spectra of **7-PE$_n$** and **7-PE-Naph**. Conditions: 1.0 × 10^{-5} M in $CHCl_3$, 25 °C. λ_{ex} = 278.5 nm (**7-PE$_1$**), 278 nm (**7-PE$_2$**), 279 nm (**7-PE$_3$**, **7-PE$_{Me}$**), 278.5 nm (**7-PE$_{butyne}$**), 278 nm (**7-PE-Naph**). (c) CPL spectra of **6-PE$_n$**. Conditions: 1.0 × 10^{-5} M in $CHCl_3$, 25 °C. λ_{ex} = 274 nm (**6-PE$_1$**, **6-PE$_2$**), 277 nm (**6-PE$_3$**), 286 nm (**6-PE$_{Me}$**), 282 nm (**6-PE$_{butyne}$**). (d) FL spectra of **6-PE$_n$** and **6-PE-Naph**. Conditions: 1.0 × 10^{-5} M in $CHCl_3$, 25 °C. λ_{ex} = 284 nm (**6-PE$_1$**, **6-PE$_2$**), 286.5 nm (**6-PE$_3$**), 276 nm (**6-PE$_{Me}$**), 282.5 nm (**6-PE$_{butyne}$**), 279 nm (**6-PE-Naph**). (e) Summary of the photophysical properties of (*S*)-**7-PE$_n$**, **7-PE-Naph**, (*S*)-**6-PE$_n$**, and **6-PE-Naph**.

Table 1 Characteristic features relevant to the electronic transition from the excited to the ground state ($S_1 \rightarrow S_0$) calculated at the RI-CC2/def2-TZVP level

Compound	ϕ_g (°)	ϕ_{ex} (°)	μ (10^{-18} esu cm)	m (10^{-20} esu cm)	$\theta_{\mu m}$ (°)	g_{lum} (calc)	g_{lum} (exp)
7-PE$_1$	51.9	38.7	2.23	6.09	80.5	9.0 × 10^{-3}	5.6 × 10^{-3}
6-PE$_1$	58.6	33.2	4.37	2.67	97.8	−1.7 × 10^{-3}	−1.8 × 10^{-3}

ϕ_g: Dihedral angle of the binaphthyl in the ground state. Calculated at the CC2/def2-TZVP level. ϕ_{ex}: Dihedral angle of the binaphthyl in the excited state. μ: Electric transition dipole moment in the excited state. m: Magnetic transition dipole moment in the excited state. $\theta_{\mu m}$: Angle of vectors between μ and m. g_{lum} (calc): Theoretically calculated g_{lum} value. g_{lum} (exp): Experimentally observed g_{lum} value.

adjustment renders the binaphthyl moieties more planar in the excited state, facilitating enhanced interaction between the naphthalene groups compared with that in the ground state.

The theoretical calculations also assessed the electric (μ) and magnetic (m) transition dipole moments in the excited state, relevant for the g_{lum} values, approximately derived for isotropic solutions as 4 ($|\mu|\ |m|\ \cos\theta_{\mu m}$)/($|\mu|^2 + |m|^2$), where $\theta_{\mu m}$ represents the angle between μ and m. The angles $\theta_{\mu m}$ for **7-PE$_1$** and **6-PE$_1$** deviated by 9.5° less and 7.8° more than 90°, respectively. Thus, the deviation from a right angle was primarily responsible for the reversal in CPL sign between **7-PE$_n$** and **6-PE$_n$**.

To further understand why the orientation of $\theta_{\mu m}$ varies dramatically spanning a right angle between **7-PE$_1$** and **6-PE$_1$**, we examine in detail the relationship between molecular structures and the orientations of μ and m (see Fig. 4 and 5). During the $S_1 \rightarrow S_0$ transition, when electrons move from the upper to the lower **PE-Naph** unit, μ is directed upwards, indicating the opposite direction to the electron movement (Fig. 4b and 5b). In a classical explanation, the generated current flows in the opposite direction to the electron movement. Thus, it is expected that the instantaneous current (i)[16,22] generated by μ during an electron transition in these molecular systems will flow along μ (from the lower to upper **PE-Naph** units), as indicated by the red arrows in Fig. 4a and 5a. Importantly, in **7-PE$_1$**, the current flows counterclockwise relative to the origin-μ axis (Fig. 4c), and clockwise in **6-PE$_1$** (Fig. 5c). Despite similar directions of electron movement from the upper to lower **PE-Naph** units in both **7-PE$_1$** and **6-PE$_1$**, the direction of current rotation is apparently reversed. According to the classic loop model (Fig. 4e), the reversal in current-flow rotation inversely affects the direction of m. Consequently, this reversal in current rotation and thus in orientation of m between **7-PE$_1$** and **6-PE$_1$** accounts for the angle $\theta_{\mu m}$ being acute in **7-PE$_1$** and obtuse in **6-PE$_1$** (Fig. 4d and 5d). Thus, **7-PE$_1$** exhibited left-handed CPL, while **6-PE$_1$** showed right-handed CPL. Additionally, the more pronounced coil-like flow of current in **7-PE$_1$** results in a larger m and thus a higher g_{lum} value compared to that in **6-PE$_1$** (compare Fig. 4d and 5d).

Our rationale may aid in understanding the structure–property relationship of m, especially for C_2-symmetric molecules like **7-PE$_1$** and **6-PE$_1$**, where the $S_1 \rightarrow S_0$ transition mainly involves LUMO → HOMO transitions. Since the value of m depends on the position of the origin, it is recommended to place the origin, in this case, in the middle of the electric current flow (or thereabout) for better analysis of the correlation between the electric current flow and m. Similarly, this reasoning would explain why compounds such as **3-PE$_1$**, **4-PE$_1$**, **5-PE$_1$**, and **8-PE$_1$** also exhibit negative CPL like **6-PE$_n$** (see Fig. S3–S6, ESI†).

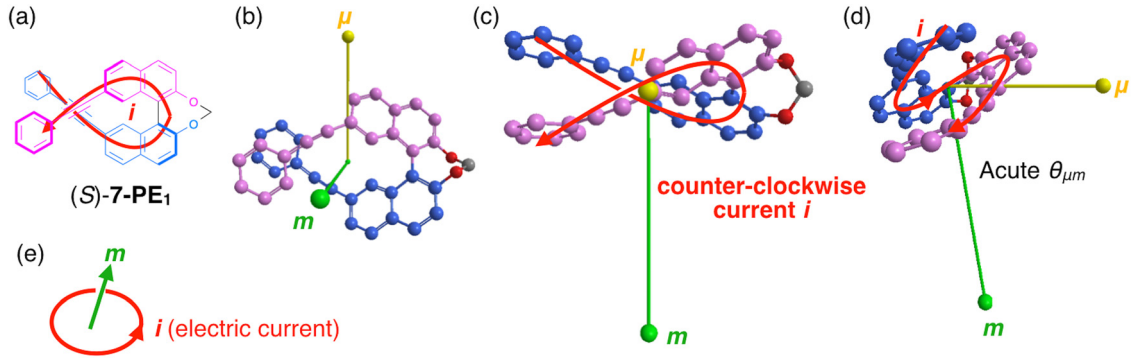

Fig. 4 (a) Expected electric current flow (*i* is shown in red) for the $S_1 \rightarrow S_0$ transitions for (*S*)-**7-PE$_1$**. (b) Electric (μ is shown in yellow) and magnetic (*m* is shown in green) transition dipole moments for the $S_1 \rightarrow S_0$ transitions for (*S*)-**7-PE$_1$**. For clarity, the relative length of *m* is magnified by 137 times compared with that of μ. (c) Top view from the direction of μ. The current flows counterclockwise relative to the origin-μ axis. (d) Side view from the direction of μ. The $\theta_{\mu m}$ is clearly acute. (e) Relationship between electric current and *m* according to the classic loop model.

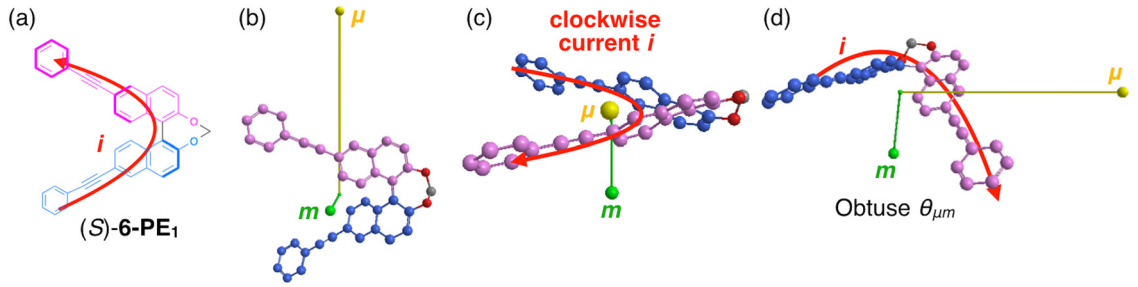

Fig. 5 (a) Expected electric current flow (*i* is shown in red) for the $S_1 \rightarrow S_0$ transitions for (*S*)-**6-PE$_1$**. (b) Electric (μ is shown in yellow) and magnetic (*m* is shown in green) transition dipole moments for the $S_1 \rightarrow S_0$ transitions for (*S*)-**6-PE$_1$**. For clarity, the relative length of *m* is magnified by 137 times compared with that of μ. (c) Top view from the direction of μ. The current flows clockwise relative to the origin-μ axis. (d) Side view from the direction of μ. Note that $\theta_{\mu m}$ is clearly obtuse.

As mentioned above, among the **6-PE$_n$** series, the g_{lum} value of **6-PE$_1$** exhibited a significantly higher value, while the g_{lum} values of **7-PE$_n$** were considerably influenced by the linker groups (Fig. 3e). Interestingly, **6-PE$_1$** has a helicene-like twisted structure in the excited state (Fig. 6c), while in the ground state, it bears the typical binaphthyl conformation. Indeed, the trend in the degree of torsional angles considerably differs in these systems (ϕ and ϕ'/ϕ'' in Fig. 6a). Both **7-PE$_1$** and **6-PE$_{Me}$** having typical binaphthyl conformations in the excited state show angles of 39° and 9/9° or 65° and 3/3°, respectively (Fig. 6b and d). In contrast, these angles were found to be 33° and 31/20° in **6-PE$_1$**, resulting in a greatly twisted conformation similar to that of a typical helicene structure.[23] This unexpected structural change in the excited state of **6-PE$_1$** is most likely responsible for its red-shifted emission and better g_{lum} value compared with the other **6-PE$_n$** derivatives.

Conclusions

The introduction of PE groups at the 6,6′- or 7,7′-positions of the (*S*)-binaphthyl backbone results in oppositely signed CPL responses. While the methylene-tethered **7-PE$_1$** and **6-PE$_1$** derivatives display superior g_{lum} values, a uniform sign inversion is observed across all related derivatives. Theoretical

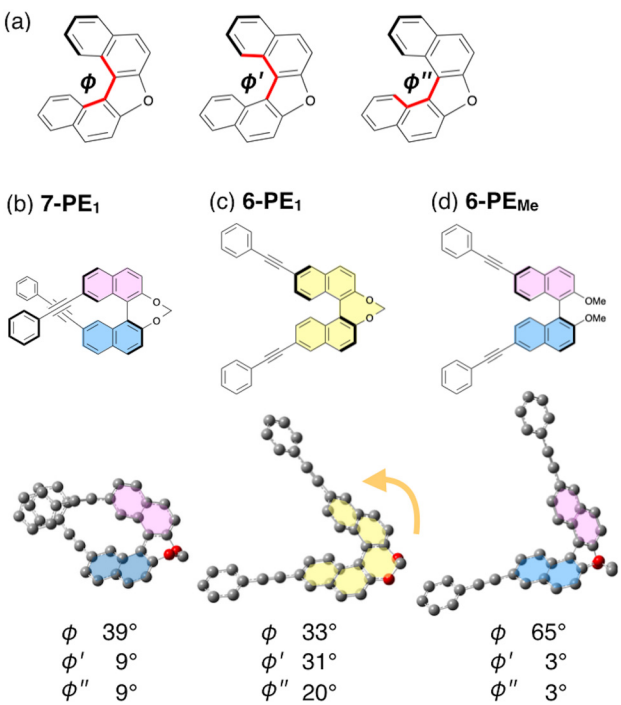

Fig. 6 (a) Definition of torsional angles (φ, φ' and φ'') of binaphthyls. Optimized structures in the excited state and the corresponding angles for (b) **7-PE$_1$**, (c) **6-PE$_1$** and (d) **6-PE$_{Me}$**.

calculations provided a rationale for the sign inversion based on the orientations of μ and m, as well as other differences in chiroptical responses.

Further analysis revealed that the direction of instantaneous current-flow rotation during transitions can reverse the orientation of m, thereby reversing the CPL sign. Previously, the properties of m were elusive, but for C_2-symmetric molecules like ours, where the major $S_1 \rightarrow S_0$ transition involves LUMO $\rightarrow$ HOMO transitions, the orientation of m can be predicted directly from the chemical structure. If μ represents the directionality of electron movement during transitions, *i.e.*, the ''difference'' in electron presence before and after transitions, then m could perhaps be represented as the ''path'' of electron movement based on current flow during the transition.

While this approach may not be universally applicable, we anticipate that our observations and the insights derived from our detailed structural analyses of binaphthyls in the excited state will contribute to the understanding and design of other novel CPL phenomena.

Author contributions

A. Imayoshi contributed to the conceptualization and methodology, and wrote the original draft of the manuscript. K. Tsubaki managed the overall project administration, provided supervision, and was responsible for the review and editing of the manuscript. S. Fujio, Y. Nagaya, and M. Sakai played major roles in the investigation. A. Terazawa, M. Sakura, K. Okada, and T. Kimoto supported the investigation. T. Mori contributed to software and investigation, and also reviewed and edited the manuscript. Y. Imai provided resources and conducted investigations. M. Hada contributed to conceptualization, methodology and software, and reviewed and edited the manuscript.

Data availability

All synthetic procedures and/computational/analytical data related to this article are provided in the ESI.†

Conflicts of interest

There are no conflicts to declare.

Acknowledgements

The authors are grateful to Prof. Keiji Hirose and Dr Rika Miyake (Graduate School of Engineering Science, Osaka University), Prof. Yasunao Hattori (Center for Instrumental Analysis, Kyoto Pharmaceutical University) and Prof. Takumi Furuta (Laboratory of Pharmaceutical Chemistry, Kyoto Pharmaceutical University), and Prof. Makoto Oba and Dr Tomohiro Umeno (Graduate School of Medical Science, Kyoto Prefectural University of Medicine) for the HRMS measurements. This study was carried out using the FT-ICR mass spectrometer and the NMR spectrometer in the Joint Usage/Research Center at the Institute for Chemical Research, Kyoto University. The computation was performed using Research Center for Computational Science, Okazaki, Japan (Project: 23-IMS-C043). This study was supported in part by Japan Society for the Promotion of Science (JSPS) KAKENHI (No. 24K18254, 22K15256, 19K23803, 22H02746 and 19H03355), Japan Science and Technology Agency (JST) CREST (JPMJCR2001), and Grant-in-Aid from the Naito Foundation. We also thank Dr Jay Freeman at Edanz for editing a draft of this manuscript.

Notes and references

1 (*a*) J. R. Brandt, F. Salerno and M. J. Fuchter, *Nat. Rev. Chem.*, 2017, **1**, 1; (*b*) Y. Sang, J. Han, T. Zhao, P. Duan and M. Liu, *Adv. Mater.*, 2020, **32**, e1900110; (*c*) Y. Deng, M. Wang, Y. Zhuang, S. Liu, W. Huang and Q. Zhao, *Light: Sci. Appl.*, 2021, **10**, 1; (*d*) J. Han, S. Guo, H. Lu, S. Liu, Q. Zhao and W. Huang, *Adv. Opt. Mater.*, 2018, **6**, 1800538; (*e*) X. Wang, S. Ma, B. Zhao and J. Deng, *Adv. Funct. Mater.*, 2023, **33**, 2214364; (*f*) Y. Yang, N. Li, J. Miao, X. Cao, A. Ying, K. Pan, X. Lv, F. Ni, Z. Huang, S. Gong and C. Yang, *Angew. Chem., Int. Ed.*, 2022, **61**, e202202227; (*g*) D.-W. Zhang, M. Li and C.-F. Chen, *Chem. Soc. Rev.*, 2020, **49**, 1331; (*h*) I. Song, J. Ahn, H. Ahn, S. H. Lee, J. Mei, N. A. Kotov and J. H. Oh, *Nature*, 2023, **617**, 92; (*i*) L. E. MacKenzie and R. Pal, *Nat. Rev. Chem.*, 2020, **5**, 109; (*j*) Y. Shi, J. Han, X. Jin, W. Miao, Y. Zhang and P. Duan, *Adv. Sci.*, 2022, **9**, e2201565.

2 (*a*) Y. Nojima, M. Hasegawa, N. Hara, Y. Imai and Y. Mazaki, *Chem. – Eur. J.*, 2021, **27**, 5923; (*b*) K. Miki, T. Noda, M. Gon, K. Tanaka, Y. Chujo, Y. Mizuhata, N. Tokitoh and K. Ohe, *Chem. – Eur. J.*, 2019, **25**, 9211; (*c*) K. Takaishi, S. Murakami, F. Yoshinami and T. Ema, *Angew. Chem., Int. Ed.*, 2022, **61**, e202204609; (*d*) W. Duan, K. Li, H. Ji, Y. Huo, Q. Yao, H. Liu and S. Gong, *Dyes Pigm.*, 2021, **193**, 109538; (*e*) Z. Jiang, X. Wang, J. Ma and Z. Liu, *Sci. China: Chem.*, 2019, **62**, 355; (*f*) J. Han, Y. Shi, X. Jin, X. Yang and P. Duan, *Chem. Sci.*, 2022, **13**, 6074; (*g*) H. Feng, J. Pu, S. Wang, S. Jiang, W. Yang, D. Cao and Y.-S. Feng, *Dyes Pigm.*, 2023, **217**, 111422; (*h*) F. Song, Z. Xu, Q. Zhang, Z. Zhao, H. Zhang, W. Zhao, Z. Qiu, C. Qi, H. Zhang, H. H. Y. Sung, I. D. Williams, J. W. Y. Lam, Z. Zhao, A. Qin, D. Ma and B. Z. Tang, *Adv. Funct. Mater.*, 2018, **28**, 1800051; (*i*) Y. Wang, X. Li, F. Li, W.-Y. Sun, C. Zhu and Y. Cheng, *Chem. Commun.*, 2017, **53**, 7505; (*j*) Q. Ye, D. Zhu, L. Xu, X. Lu and Q. Lu, *J. Mater. Chem.*, 2016, **4**, 1497.

3 Z.-B. Sun, J.-K. Liu, D.-F. Yuan, Z.-H. Zhao, X.-Z. Zhu, D.-H. Liu, Q. Peng and C.-H. Zhao, *Angew. Chem., Int. Ed.*, 2019, **58**, 4840.

4 K. Takaishi, F. Yoshinami, Y. Sato and T. Ema, *Chem. – Eur. J.*, 2024, e202400866.

5 K. Takaishi, K. Iwachido, R. Takehana, M. Uchiyama and T. Ema, *J. Am. Chem. Soc.*, 2019, **141**, 6185.

6 J. Li, C. Hou, C. Huang, S. Xu, X. Peng, Q. Qi, W.-Y. Lai and W. Huang, *Research*, 2020, **2020**, 3839160.

7 (*a*) Y. He, S. Lin, J. Guo and Q. Li, *Aggregate*, 2021, **2**, e141; (*b*) S. Yang, F. Li, Q. Li, J. Han and Y. Cheng, *ACS Appl. Opt. Mater.*, 2023, **1**, 1492.
8 Y. Zhang, H. Li, Z. Geng, W.-H. Zheng, Y. Quan and Y. Cheng, *ACS Nano*, 2022, **16**, 3173.
9 (*a*) N. F. M. Mukthar, N. D. Schley and G. Ung, *J. Am. Chem. Soc.*, 2022, **144**, 6148; (*b*) Y. Zhou, H. Li, T. Zhu, T. Gao and P. Yan, *J. Am. Chem. Soc.*, 2019, **141**, 19634.
10 (*a*) Z. Geng, Y. Zhang, Y. Zhang, Y. Li, Y. Quan and Y. Cheng, *J. Mater. Chem.*, 2021, **9**, 12141; (*b*) Z. Geng, Y. Zhang, Y. Zhang, Y. Quan and Y. Cheng, *Angew. Chem., Int. Ed.*, 2022, **61**, e202202718.
11 (*a*) Y. Nojima, M. Hasegawa, N. Hara, Y. Imai and Y. Mazaki, *Chem. Commun.*, 2019, **55**, 2749; (*b*) T. Sato, N. Tajima, H. Ueno, T. Harada, M. Fujiki and Y. Imai, *Tetrahedron*, 2016, **72**, 7032; (*c*) T. Kinuta, N. Tajima, M. Fujiki, M. Miyazawa and Y. Imai, *Tetrahedron*, 2012, **68**, 4791; (*d*) T. Kimoto, N. Tajima, M. Fujiki and Y. Imai, *Chem. Asian J.*, 2012, **7**, 2836.
12 K. Takaishi, T. Matsumoto, M. Kawataka and T. Ema, *Angew. Chem., Int. Ed.*, 2021, **60**, 9968.
13 (*a*) K. Takaishi, S. Murakami, K. Iwachido and T. Ema, *Chem. Sci.*, 2021, **12**, 14570; (*b*) D. Kaji, S. Ikeda, K. Takamura, N. Tajima, M. Shizuma, T. Mori, M. Miyasaka and Y. Imai, *Chem. Lett.*, 2019, **48**, 874; (*c*) T. Amako, T. Kimoto, N. Tajima, M. Fujiki and Y. Imai, *RSC Adv.*, 2013, **3**, 6939; (*d*) N. Hara, D. Kaji, K. Okuda, M. Shizuma, N. Tajima and Y. Imai, *Chem. Lett.*, 2018, **47**, 894; (*e*) K. Nakabayashi, S. Kitamura, N. Suzuki, S. Guo, M. Fujiki and Y. Imai, *Eur. J. Org. Chem.*, 2016, 64.
14 (*a*) Y. Imai, *Chem. Lett.*, 2021, **50**, 1131; (*b*) Y. Sheng, D. Shen, W. Zhang, H. Zhang, C. Zhu and Y. Cheng, *Chem. – Eur. J.*, 2015, **21**, 13196; (*c*) T. Kimoto, T. Amako, N. Tajima, R. Kuroda, M. Fujiki and Y. Imai, *Asian J. Org. Chem.*, 2013, **2**, 404; (*d*) K. Nakabayashi, T. Amako, N. Tajima, M. Fujiki and Y. Imai, *Chem. Commun.*, 2014, **50**, 13228; (*e*) Y. Li, C. Xue, M. Wang, A. Urbas and Q. Li, *Angew. Chem., Int. Ed.*, 2013, **52**, 13703; (*f*) H. Okada, N. Hara, D. Kaji, M. Shizuma, M. Fujuiki and Y. Imai, *Phys. Chem. Chem. Phys.*, 2020, **22**, 13862.
15 (*a*) K. Takaishi, K. Iwachido and T. Ema, *J. Am. Chem. Soc.*, 2020, **142**, 1774; (*b*) S. Nakanishi, N. Hara, N. Kuroda, N. Tajima, M. Fujiki and Y. Imai, *Org. Biomol. Chem.*, 2018, **16**, 1093; (*c*) M. Okazaki, T. Mizusawa, K. Nakabayashi, M. Yamashita, N. Tajima, T. Harada, M. Fujiki and Y. Imai, *J. Photochem. Photobiol., A*, 2016, **331**, 115.
16 R. G. Uceda, C. M. Cruz, S. Miguez-Lago, L. A. de Cienfuegos, G. Longhi, D. A. Pelta, P. Novoa, A. J. Mota, J. M. Cuerva and D. Miguel, *Angew. Chem., Int. Ed.*, 2024, **63**, e202316696.
17 M. Sakai, S. Fujio, A. Imayoshi, T. Sasamori, K. Okada, Y. Imai, M. Hasegawa and K. Tsubaki, *Chem. – Asian J.*, 2024, e202400159.
18 (*a*) K. Ma, W. Chen, T. Jiao, X. Jin, Y. Sang, D. Yang, J. Zhou, M. Liu and P. Duan, *Chem. Sci.*, 2019, **10**, 6821; (*b*) K. Takaishi, S. Hinoide, T. Matsumoto and T. Ema, *J. Am. Chem. Soc.*, 2019, **141**, 11852; (*c*) Y. Wang, Q. Liao, Y. Feng and Q. Meng, *J. Mol. Struct.*, 2024, **1304**, 137695; (*d*) Y. Wang, Y. Li, S. Liu, F. Li, C. Zhu, S. Li and Y. Cheng, *Macromolecules*, 2016, **49**, 5444; (*e*) T. Ikai, N. Mishima, T. Matsumoto, S. Miyoshi, K. Oki and E. Yashima, *Angew. Chem., Int. Ed.*, 2024, **63**, e202318712; (*f*) W. Huang, Y. Zhu, K. Zhou, L. Chen, Z. Zhao, E. Zhao and Z. He, *Chem. – Eur. J.*, 2023, e202303667; (*g*) S. Jena, A. Thayyil Muhammed Munthasir, S. Pradhan, M. Kitahara, S. Seika, Y. Imai and P. Thilagar, *Chem. – Eur. J.*, 2023, **29**, e202301924.
19 K. Zhang, J. Zhao, N. Zhang, J.-F. Chen, N. Wang, X. Yin, X. Zheng and P. Chen, *J. Mater. Chem.*, 2022, **10**, 1816.
20 TURBOMOLE V7.8 2023, a development of University of Karlsruhe and Forschungszentrum Karlsruhe GmbH, 1989-2007, TURBOMOLE GmbH, since 2007; available from **https://www.turbomole.org**.
21 (*a*) C. Hättig and A. Köhn, *J. Chem. Phys.*, 2002, **117**, 6939; (*b*) F. Weigend and R. Ahlrichs, *Phys. Chem. Chem. Phys.*, 2005, **7**, 3297; (*c*) F. Weigend, *Phys. Chem. Chem. Phys.*, 2006, **8**, 1057.
22 (*a*) M. Fortino, G. Schifino and A. Pietropaolo, *Chirality*, 2023, **35**, 673; (*b*) F. Furche, R. Ahlrichs, C. Wachsmann, E. Weber, A. Sobanski, F. Vögtle and S. Grimme, *J. Am. Chem. Soc.*, 2000, **122**, 1717.
23 P. Ravat, R. Hinkelmann, D. Steinebrunner, A. Prescimone, I. Bodoky and M. Juríček, *Org. Lett.*, 2017, **19**, 3707.

